Journal of Solid Mechanics Vol. 15, No. 1 (2023) pp. 78-89
DOI: 10.22034/jsm.2022.1935745.1705

Research Paper

A Distributed Parameters Model for Broadband Energy Harvesting From Nonlinear Vibration of the Piezoelectric System

M.M. Zamani, M. Abbasi *, F. Forouhandeh

Department of Engineering, Shahrood Branch , Islamic Azad University, Shahrood, Iran

Received 1 November 2022; accepted 4 January 2023

ABSTRACT

To the extent of the usable bandwidth of the piezoelectric energy harvesters (PEH) and progress the harvesting proficiency, a 2-DOF bistable PEH (2D-BPEH) with an elastic substructure is developed to show the strengthened nonlinear large-amplitude periodic vibration performances. Introducing the substructure, which is demonstrated by the mass-spring sub-system added between the distributed bimorph beam and exciting base, dynamic motions of the beam is expected to reproduce high energy trajectories and large deflections. Due to raising the accuracy of the model and results, the key novelty of the present study is to consider the mathematical model of composite smart bimorph beam with the aid of distributed parameters model and Von Karman strain relations. With the help of Hamilton's principle, Electro mechanic modeling of the 2-DOF system has been derived and three coupled equations are consequent utilizing the Galerkin method. Primarily deflection and voltage frequency response curves are calculated analytically; then, the model has been compared and validated by the results of the 2-DOF PEH model with lumped parameter beam in the literature. Numerical results indicate that accurate designing of 2-DOF piezoelectric energy harvester parameters could intensely enhance the generating voltage and at a broader exciting frequency band. The results have shown that the 2-DOF bistable PEH coupled with elastic substructure as a magnifier harvests extra electrical power at specific input frequencies and operates at larger bandwidth than routine PEHs.

Keywords : 2D-BPEH; Distributed parameter model; Nonlinear vibration; Harvesting voltage; Time and frequency responses.

1 INTRODUCTION

DURING the last decade, with the progress of electromechanics model and mechanisms [1]-[4] and integrated energy harvesting systems and medical implants, e.g., leadless peacemakers, numerous research studies have

*Corresponding author. Tel.: +98 9151250720.
E-mail address: m.abbasi28@yahoo.com (M.Abbasi)

focused on piezoelectric energy harvester units, which convert mechanical energy into electricity using piezoelectric elements [5]. Between lots of energy sources, energy harvesting from mechanical vibration has developed wide-ranging because of availability [6]; also, harvesting from the ambient vibrations is much considered since current electrical devices require little power and energy [7]. Most of the previous PEHs are constructed based on resonance in linear systems, resulting in problems like high sensitivity to frequency band uncertainty. Linear systems, the device's performance is limited to a narrowband frequency which was hard to achieve in practical operations. In order to broadband operating frequencies, scientists have developed several solutions, including tuning method, multi-model method, and nonlinear method [8]-[10]. Between these approaches, the nonlinear method has mostly significant effect on extending the operating bandwidth. This technique introduces nonlinear factors into a linear system, converts its motion equation of a single solution into a multi-solution nonlinear equation , subsequently moves the peaks and significantly changes the bandwidth characteristic [11],[12]. One of the advantages of a nonlinear system is the existence of multiple equilibrium points in them. Considering the nonlinearity in the system allows receiving a significant amplitude response in a broader range of frequencies. Newly scientists have used nonlinear methods to make energy harvesting available in a broadband frequencie extensively [13] .Yang et al. [14] analyzed PEH contain nonlinear geometric factors and proved that increasing the nonlinear coefficient raises harvested voltage. Jahani et al. [15] considered PEH with nonlinear terms such as geometric nonlinearity and demonstrated that the nonlinear factors lead to increasing the maximum harvested electrical power. Lin [16] appealed that the harvesting power of a piezoelectric cantilever beam excited by a random noise source can be enhanced by repulsive magnetic force. Between the nonlinear techniques, the BPEH can produce a significant amplitude motion of chaotic motion at various excitation using broadening the bandwidth significantly [17]. In general, beam-type bistable oscillators have a double-well restoring force potential that provides three separate inter-well dynamic regimes (e.g., low-energy vibration, chaotic and high-energy periodic vibration), depending on the input amplitude [18]. One of the most familiar arrangements for BPEH is magnetic repulsion harvester in which the nonlinearity governed by the repulsion force can significantly increase the harvesting power [19]. Gammaitoni et al. [20] presented a bistable PEH configuration and calculated the effect of magnet spacing on the output voltage. Erturk et al. [21] showed that the bistable PEH excited by harmonic inputs could show large amplitude periodic or chaotic motions. Bistable PEH improves eight times in harvested power compared with linear ones. Ferrari et al., [22] compared the displacement response of a BPEH under band-limited excitation and confirmed the results by tests. Stanton et al. [23],[24] considered the performance of a BPEH by numerical and experimental methods. They established a horizontally placed bistable model and studied the influence of different structural parameters on the system output, e.g., amplitude and frequency of the excitation. Karami and Inman [25] considered the perturbation method for BPEH in the initial resonance state. Erturk et al. [26] considered another BPEH structure with cantilever beams. The results illustrate that the output power is eight times the linear system. Nevertheless, the good profits of BPEHs, there is still a chance for improvement. One significant challenge is an operative technique to make the oscillations in a high-energy trajectory to increase the PEH performance. To progress the outpower of PEH under low-level excitation, investigators have tried to make them vibrate with large-amplitude inter-well motion. Sebald et al, [27],[28] initiate that an external intrusion can help BPEH return to a large-amplitude motion state, and raising the excitation level may help them to change weak low-amplitude orbits to a large-amplitude motion. Kim and Seok [29] planned multi-stable PEH, having thinner and broader potential wells compared with BPEH, thus allowing them to extract power in broadband frequencies, even at low excitation levels. Novel 2-DOF BPEH is presented by Zhao et al, [30] are composed of two cantilever beams and mass blocks, which could makes the oscillations supplementary stable.There have been essential concern paid to structures coupled with elastic substructures. The magnifier substructure is planned to supply an advance for the BPEH. Its tasks by leading high-energy motion and enlarged output performance. However, some arrangements of elastic magnifiers that are generally displayed as a linear mass-spring system positioned between the bimorph beam and the base. Vasic et al, [31] developed a double beam harvester with a magnifier to investigate the added harvesting power to a traditional harvester. Similarly, Wang et al, [32] studied an effective PEH including an elastic substrate. Zhou et al, [33] proposed an innovative PEH with a multi-mode magnifier, which is capable of significantly increasing the bandwidth and harvesting energy from ambient vibrations. Aldraihem et al. [34] developed an energy harvester coupled with a mass-spring magnifier, their results are also consistent with increased power output and a broader bandwidth process. In order to increase harvesting power, Aladwani et al, [35] analyzed a PEH containing a simple spring magnifier using finite element theory, the suggested harvester enhanced power output and broad the bandwidth by about 21%. An improved prototype for cantilevered PEH with a tip mass offset and magnifier are reported by Tang et al, [36]. They also investigated a series of MDOF harvesters that resemble a flexible magnifier attached with a bimorph beam [37]. Wang et al, [38] investigated a BPEH with a flexible magnifier and derived the equations using a 2-DOF lumped parameter model.

Due to the influence of the distributed mass of the cantilever structure on the exciting amplitude, the results of the lumped model are inaccurate. To the best of authors information , There is not similar study by considering the mathematical model of composite smart bimorph beam by means of distributed parameters model and von karman strain relations. Consequently for increasing the accuracy of the model and results, the present study attentions essentially on the development of a BPEH with a magnifier using distributed parameter model including von-Karman strains. The system is analytically solved to examine the harvested voltage and vibration of the PEH.

2 ANALYTICAL MODELING AND EQUATIONS

2.1 Modeling and Hamilton principle

Fig. 1 illustrates the configuration scheme of 2-DOF PEH involves a cantilever bimorph beam, including a core layer covered by two piezoelectric faces and resting on an elastic substructure. L, b, h_s, and h_p are beam length, width, core thickness, and piezoelectric layer height, respectively. The magnifier substructure is modeled by the equivalent mass M_b and equivalent stiffness K_b. As shown in Fig.1, this bistable energy harvester comprises a couple of magnets of mass and inertia M_t and I_t , respectively. Also, z_b and z_m are the amplitudes of base excitation and magnifier motion respectively; additionally, distributed vibrations of the cantilever beam are $w(x,t)$. To obtain equilibrium equations for the distributed parameter system using the Hamilton principle, one can write:

$$\int_{t_1}^{t_2}[\delta(T-U)+\delta W]dt=0 \tag{1}$$

T,U, and W are the total kinetic energy, total potential energy, and the work done by the external loads, respectively. The kinetic energy of the system can be written as $T=T_1+T_2+T_3$; where T_1,T_2 and , T_3 represent the kinetic energy of the beam, the elastic substructure and the moving tip magnet, respectively. These energy components are as follows:

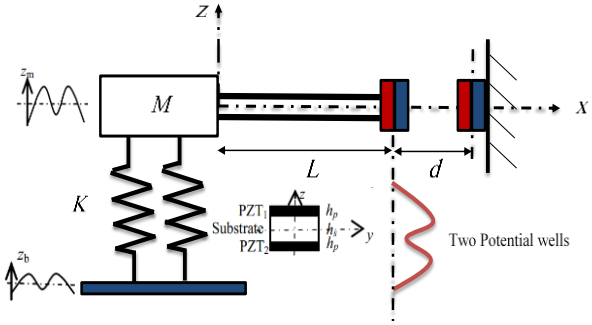

Fig.1
Configuration of bistable PEH with magnifier substructure.

$$T_1=\frac{1}{2}\int_{V_s}^{0}\left[\frac{\partial[Z_m(t)+w(x,t)]}{\partial t}\right]^2 dV_s+\sum_{i=1}^{2}\frac{1}{2}\int_{V_{pi}}^{0}\rho_{pi}\left[\frac{\partial[Z_m(t)+w(x,t)]}{\partial t}\right]dV_{pi} \tag{2}$$

where ρ_s and ρ_{pi} are the density of the core and piezo faces, respectively and $i,(i=1,2)$ used for two faces layers of the bimorph beam. Furthermore:

$$T_2=\frac{1}{2}\int_{V_s}^{0}\left[\frac{\partial[Z_m(t)+w(x,t)]}{\partial t}\right]^2 dV_s+\frac{1}{2}I_t\left[\frac{\partial w^2(L,t)}{\partial x\,\partial t}\right]^2 \tag{3}$$

$$T_3=\frac{1}{2}M_b Z_m(t)^2 \tag{4}$$

The total potential energies of the harvester are: $U = U_1 + U_2 + U_3 + U_4$. In which U_1 and U_2 are the strain energies of the beam and flexible magnifier, respectively, besides U_3 and U_4 are stored energy of the electrical circuit and nonlinear potential generated by the repulsive magnetic forces, respectively. The strain energy of the beam and magnifier are:

$$U_1 = \frac{1}{2}\int_{V_s}^{0} \varepsilon_s \sigma_s dV_s + \frac{1}{2}\sum_{i=1}^{2} \varepsilon_{pi} \sigma_{pi} dV_{pi} \tag{5}$$

$$U_2 = \frac{1}{2} K_b Z_m^2 \tag{6}$$

σ_s and ε_s are stress and strain of the core, similarly σ_p and ε_p are the stress, and strain of both piezoelectric faces, respectively. Consuming Bernoulli beam and von-Karman strains .One of the central constructional relations of piezoelectric materials are as follows:

$$\begin{aligned} T_p &= C^E \varepsilon_p - e_{31} E_z \\ D_z &= e_{31} \varepsilon_p + \varepsilon_{33}^s E_z \end{aligned} \tag{7}$$

where E_z and D_z characterize the electric field and displacement in the *z*-direction, correspondingly. Also e_{31} is the piezoelectric constant, C^E is the elastic modulus of the material and ε_{33}^s is the piezoelectric permittivity. Substituting this relation in the Eq. (7) the strain energy of piezoelectric layers is equal to:

$$\sum_{i=1}^{2}\int_{V_{pi}}^{0} \varepsilon_{pi} \sigma_{pi} dV_{pi} = \sum_{i=1}^{2}\int_{V_p}^{0} \varepsilon_{pi} (C^E \varepsilon_{pi} - e_{31} E_Z) dV_{pi} \tag{8}$$

The Electrical energy at both piezoelectric layers is:

$$U_3 = \sum_{i=1}^{2}\int_{V_{pi}}^{0} E_z D_z dV_{pi} = \frac{1}{2}\sum_{i=1}^{2}\int_{V_p}^{0} (e_{31} E_z \varepsilon_p + \varepsilon_{33}^s E_z^2) dV_{pi} \tag{9}$$

Besides the Magnetic potential created by the magnetic force are as follows, where $M_{A,B}$ and $V_{A,B}$ are the magnetic moments and volumes of each magnet, respectively [23]:

$$U_4 = \frac{\mu_0 M_A V_A M_B V_B [-w^2(x,t) + 2d^2 - 3dw(x,t) + w'(x,t)]}{4\pi\sqrt{w^2(x,t)+1}[w^2(x,t)d^2]^{2.5}} \tag{10}$$

2.2 Reduce order of equations and nondimensional form

The dynamic response of the cantilever beam be formulated using the Rayleigh-Ritz method as [39]:

$$w(x,t) = \sum_{j=1}^{N} \phi_j(x) r_j(t) = \left\{\vec{\phi}(x)\right\}\left\{\vec{r}(t)\right\} \tag{11}$$

In which $\vec{\phi}(x)$ and $\vec{r}(t)$ are the mode shape function of the beam and generalized modal coordinates, respectively. Also, *N* is the number of considered modes. Following calculations are considered the first mode vibrations (j=1) and excitations are nearby the fundamental frequency, so $w(x,t) = \phi(x) r(t)$. At fundamental mode for undamped vibration, for a cantilever beam with a tip mass, $\phi(x)$ is assumed to be [39]:

$$\phi(x)=\left[\cos\frac{\lambda}{L}x-\cosh\frac{\lambda}{L}x+\sigma\left(\sin\frac{\lambda}{L}x-\sinh\frac{\lambda}{L}x\right)\right]$$
$$\sigma=\frac{\sin\lambda-\sinh\lambda+\lambda(M_t/\rho AL)(\cos\lambda-\cosh\lambda)}{\cos\lambda-\cosh\lambda+\lambda(M_t/\rho AL)(\sin(M_t/\rho AL)-\sinh\lambda)} \tag{12}$$

where $\rho=\frac{\rho_s h_s+2\rho_p h_p}{h_s+2h_p}$ and $A=b(h_s+2h_p)$, λ is the wavelength of the oscillations. After some mathematical operation, the equations of the 2-DOF piezoelectric harvester are obtained as follows:

$$\begin{aligned}&M_0\ddot{r}+C_0\dot{r}+K_0-\alpha\upsilon-k_1r+k_3r^3+B_2\ddot{z}_m=-B_2\ddot{z}_b\\&B_1\ddot{z}_m+K_bz_m+B_2\ddot{r}=-B_1\ddot{z}_b\\&\alpha\dot{r}+C_p\dot{v}+v/R=0\end{aligned} \tag{13}$$

The coefficients of the above equations are:

$$\begin{aligned}&M_0=\int_{V_s}^{0}[\rho_s\phi^2(x)dx]+\int_{V_{pi}}^{0}[\rho_{pi}(z)\phi^2(x)dx]+\begin{bmatrix}M_t\phi^2(L)\\+I_t\phi'^2(L)\end{bmatrix}\\&K_0=\int_{V_s}^{0}C_s[-z\phi''(x)]^2dV_s+\sum_{i=1}^{2}\int_{V_{pi}}^{0}C_{11}^{E}(z)[-z\phi''(x)]^2dV_{pi}\\&B_2=\int_{V_s}^{0}\rho_s\phi(x)dV_s+\sum_{i=1}^{2}\rho_{pi}(z)\phi(x)dV_{pi}+M_t\phi(L)\\&\alpha=\sum_{i=1}^{2}\int_{V_{pi}}^{0}C_s(z)\left[-z\phi''(x)e_{31}(z)[-\nabla\psi(z)\right]dV_{pi}\\&C_p=\sum_{i=1}^{2}\int_{V_{pi}}^{0}\varepsilon_{33}^{s}(z)[-\nabla\psi_v(z)]^2dV_{pi}\\&k_1=\frac{\mu_0M_AV_AM_BV_B}{2\pi}\begin{bmatrix}6\phi^2(L)+d^2\phi'^2(L)\\+3d\phi(L)\phi'(L)\end{bmatrix}k/d^5\\&k_3=\left(\int_0^L\varphi\varphi''dx\right)\left(\int_0^L\varphi'^2dx\right)+3\mu_0M_AV_AM_BV_B\frac{\begin{bmatrix}30\phi^4(L)+13d^2\phi^2(L)\phi'^2(L)\\+20d\phi^3(L)\phi'(L)\end{bmatrix}}{8\pi d^7}\end{aligned} \tag{14}$$

The dimensionless form of Eq. (13) is as follows:

$$\begin{aligned}&\ddot{X}(\tau)+\mu\dot{X}(\tau)+(1-r)X(\tau)+X^3(\tau)+\ddot{Z}_m(\tau)-V(\tau)=-\ddot{Z}_b(\tau)\\&\ddot{Z}_m(\tau)+\alpha Z_m(\tau)+\beta\ddot{X}(\tau)=-\ddot{Z}_b(\tau)\\&k^2\dot{X}(\tau)+\dot{V}(\tau)+\theta V(\tau)=0\end{aligned} \tag{15}$$

In which the non-dimensional parameters and coefficients are defined as:

$$\begin{aligned}&\omega_0=\sqrt{K_0/M_0};\mu=\frac{C_0}{M_0\omega_0};\tau=\omega_0t;r=\frac{k_1}{K_0};l=\sqrt{K_0/k_3};r(t)=lX(\tau);\upsilon(t)=\frac{K_0lV(\tau)}{\alpha};\\&\{z_m(t),z_b(t)\}=\frac{lM_0}{B_2}\{Z_m(\tau),Z_b(\tau)\};\alpha=\frac{r_k}{1+r_m};\beta=\frac{B_2^2}{B_1M_0};\theta=\frac{1}{C_pR_L\omega_0};\chi^2=\frac{\alpha^2}{C_pK_0}\end{aligned} \tag{16}$$

where $r_m = M_b / M_{eq}, r_k = K_b / K_{eq}$ are the mass and stiffness ratios of the 2-DOF harvester, Also $K_{eq} = 3EI / L^3$ and $M_{eq} = \sum_{i=1}^{2} \int_0^{V_{pi}} \rho_{pi}(z)\phi(x)dV_{pi} + \int_0^{V_s} \rho_s \phi(x)dV_s$, where E and I are the equivalent Young's moduli and moment of inertia, respectively.

2.3 The frequency response at steady state

In this section, frequency response of the nonlinear harvester is obtained using the harmonic balance method, analytically. By assuming the harmonic base excitation equals to $\ddot{Z}_b(\tau) = F_0 \mathrm{Cos}\Omega\tau$, the first order periodic solution of the system could assume as follows:

$$\begin{aligned} X(\tau) &= \alpha_0(\tau) + \alpha_1(\tau)\mathrm{Cos}\Omega\tau + \alpha_2(\tau)\mathrm{Sin}\Omega\tau \\ V(\tau) &= b_1(\tau)\mathrm{Cos}\Omega\tau + b_2(\tau)\mathrm{Sin}\Omega\tau \end{aligned} \tag{17}$$

where Ω is the dimensionless excitation frequency; Rewriting $Z_m(\tau)$ in terms of $X(\tau)$ and $V(\tau)$ using Eq. (13), forth order differential equation of the harvester could simplify as:

$$\frac{1-\beta}{\alpha}X^{(4)} + \frac{\mu}{\alpha}X^{(3)} + \left(\frac{1-r+\alpha}{\alpha}\right)\ddot{X} + (\mu+1-s)\dot{X} + X^3 + \frac{1}{\alpha}(3\ddot{X}X^2 + 6X\dot{X}^2) - \frac{1}{\alpha}\ddot{V} - V = -\ddot{Z}_b \tag{18}$$

Substituting the above relations in the central equation and performing the mathematical operation, the frequency response relation of the beam vibrations is:

$$\left(D_1 + D_3\frac{\kappa^2\Omega\theta}{\theta^2+\Omega^2}\right)^2 + \left(D_2 - D_3\frac{\kappa^2\Omega^2}{\theta^2+\Omega^2}\right)^2 = \frac{f^2}{A^2} \tag{19}$$

In which $A^2 = a_1^2 + a_2^2$, also:

$$\begin{aligned} D_1 &= \frac{1-\beta}{\alpha}\Omega^4 - \frac{1-r+\alpha}{\alpha}\Omega^2 + 1 - r + 3\alpha_0^2 + \frac{3}{4}A^2 - \frac{3}{\alpha}\Omega^2\alpha_0^2 - \frac{3}{4\alpha}\Omega^2A^2 \\ D_2 &= \frac{\mu}{\alpha}\Omega^3 - \mu\Omega; D_3 = \frac{1}{\alpha}\Omega^2 - 1; \end{aligned} \tag{20}$$

Furthermore, the coefficients of the output voltage are:

$$b_1 = -\frac{\kappa^2\Omega}{\theta^2+\Omega^2}(\Omega\alpha_1 + \theta\alpha_2); b_2 = \frac{\kappa^2\Omega}{\theta^2+\Omega^2}(\theta\alpha_1 - \alpha_2\Omega) \tag{21}$$

3 RESULT AND DISCUSSION

3.1 Frequency response and verification

The input parameters for the electromechanics and geometric properties of the harvester are given in Table1. Also $M_t = 5.5gr$, and $d = 24mm$; further dimensionless parameters of the system are equal to: $\mu = 0.04, \kappa^2 = 0.0716,$ $\theta = 0.1349$ and $r = 1.2158$.

The evaluation and justification of the results with Ref. [38] are illustrated in Fig.2. It can be concluded that considering the system with discrete parameters, the response value of the nonlinear response curve system is larger and the results are more accurate. The reason for the differences between the two curves is the more bending of the curve in the present study (with distrbuted parameters model) because it predicts the flexibility of the beam more

accurately by considering the actual and nonlinear strains, correctly and with a larger amount than the other curve presented in the reference article (with lumped parameters model). The amount of deformation has been drawn with a little larger values due to less stiffness of beam at present study.

Table 1
Electromechanical properties of the harvester.

Properties	Piezo layers	Beam core
Young's modulus (*GPa*)	115	60.6
Density (Kg/m^3)	7900	7900
Thickness (*mm*)	0.2	0.157
Length (*mm*)	62	62
Width (*mm*)	18	18
Piezoelectric constant	1200 ε_0	-

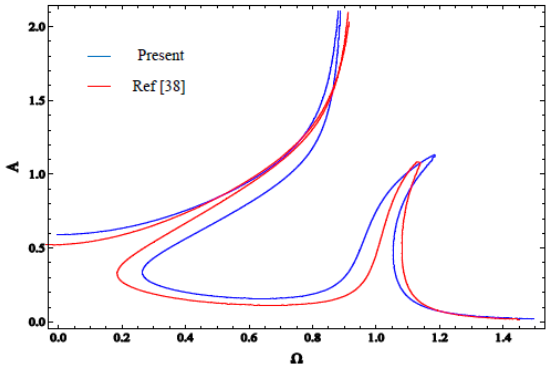

Fig.2
Validation of frequency response curves with Ref. [38]

In this subsection, the frequency-response curves and output voltage are plotted to investigate the effects of various parameters such as r_m and r_k on the harvester responses. In Figs. 3(a) and 3(b) the dimensionless frequency-response curves are plotted for vibration of tip mass and harvested voltage, respectively at different values of mass and stiffness ratios when $f = 0.05$. As we can see from the figures, there are two resonance peaks in the frequency- response of 2-DOF vibrational systems except in the harvester with no elastic substructure. Also, response curves bend to the right noticeably, because of the nonlinear magnetic force. Besides, increasing r_m and r_k, the first peak moved to the right slowly and the amplitude of these two peaks was amplified obviously. Without elastic substructure, the resonant frequency equals $\Omega = 0.85$ and the max. Of amplitude is equal to A=1.05. Besides, there are three solutions in the frequency domain $0.25 \prec \Omega \prec 0.8$, also the min and max. Responses are stable responses and the middle one is unstable. As shown in the Fig.3, when stiffness and mass ratios equal to 5, two resonant frequencies occur at 0.88 and 1.23, and the max. Vibration amplitudes equal to 2.14 and 1.21, respectively. There are three solutions for the vibration amplitude when excitation frequency bands are $0.3 \prec \Omega \prec 0.88$ or $1.1 \prec \Omega \prec 1.23$ in which these two regions have two stable responses and the harvester system is bistable. However when $\Omega \prec 0.3, \Omega \succ 1.1$ or $0.88 \prec \Omega \prec 1.23$ system has one stable responses and monostable nature. It should be noted that frequencies of 0.3 and 1.1 are called scape points. when $r_m = r_k = 25$, two frequency peaks occurred at 0.92 and 1.22, in which the max. Responses equal to 2.28 and 1.36, respectively; also, the escape points occurred at 0.3 and 1.05.

At Fig. 4, the response amplitudes are plotted versus the base excitation level for different values of the stiffness and mass ratios when $\Omega = 0.8$. In higher stiffness and mass ratios increase, two escape points occur in smaller values, Since utilizing bigger EM , when the non-dimensional excitation frequency is 0.8, decreased the hardening nonlinearity of the system so, the range of instability for excitation level (f) became narrower and system have larger stability range. Based on Fig. 4, the instability range for system without EM is equal to $0.05 < f < 0.31$. Moreover for the case $r_m = r_k = 5$, the instability range is $0.02 < f < 0.16$ and for the case $r_m = r_k = 25$, the instability range is $0.02 < f < 0.12$.

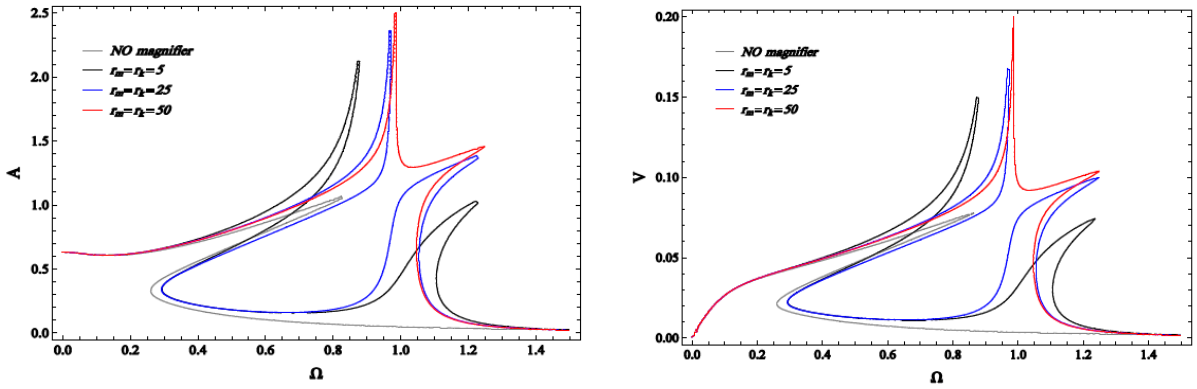

(a) (b)

Fig.3
Dimensionless response - frequency curves for different value of r_m and r_k ; (a) Vibration of the tip , (b) Harvested voltage.

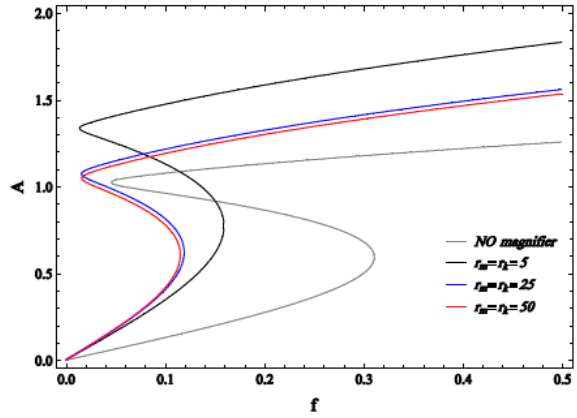

Fig.4
Beam response versus levels of the base excitation for different stiffness and mass ratios.

3.2 Time response of the harvester

In this subsection at Figs.5-7, the voltage of the 2-DOF harvester and phase plane diagram of the bimorph beam has been plotted. Figs.5 (a-c) have plotted the graphs for various excitation levels when $r_m = r_k = 50$ and $\Omega = 0.8$.

As demonstrated in the Fig.5(a), if the excitation level is microscopic, the beam oscillates about an equilibrium point with microscopic tip velocity and vibrations, causing the intra-well motion and low harvested voltage. In this case, Despite the robust elastic substructure, due to weak excitation level, the performance of 2-DOF PEH is not enough to overcome the potential barrier and show bistable motion. As shown in the Fig. 5(b), if the excitation levels increased, the output voltage is chaotic because of the chaotic motion of beam tip among two wells .Considering Fig. 5(c), by raising the excitation level more, the beam tip shows a high-energy inter-well motion, considered by a periodic oscillation with high amplitude, causing a substantial increase in the vibration amplitudes and the harvested power.

As shown in Figs. 6(a,b) output voltage and phase diagram of the 2-DOF harvester are plotted at different excitation levels when $r_m = r_k = 40$ and $\Omega = 1.1$. With a lower excitation level, there is low energy oscillating motion inside the well. However, at higher excitation level the PEH shows bistable high energy motion and harvesting voltage increased intensely.

Figs.7 (a-c) are plotted the output voltage and phase portrait diagrams of PEH for different excitation frequencies when excitation level equals to f= 0.1. As shown in these plots, by increasing the excitation frequencies toward the higher values, in which $\Omega \prec 1$,the harvester shows high amplitude bistable motions between the wells.

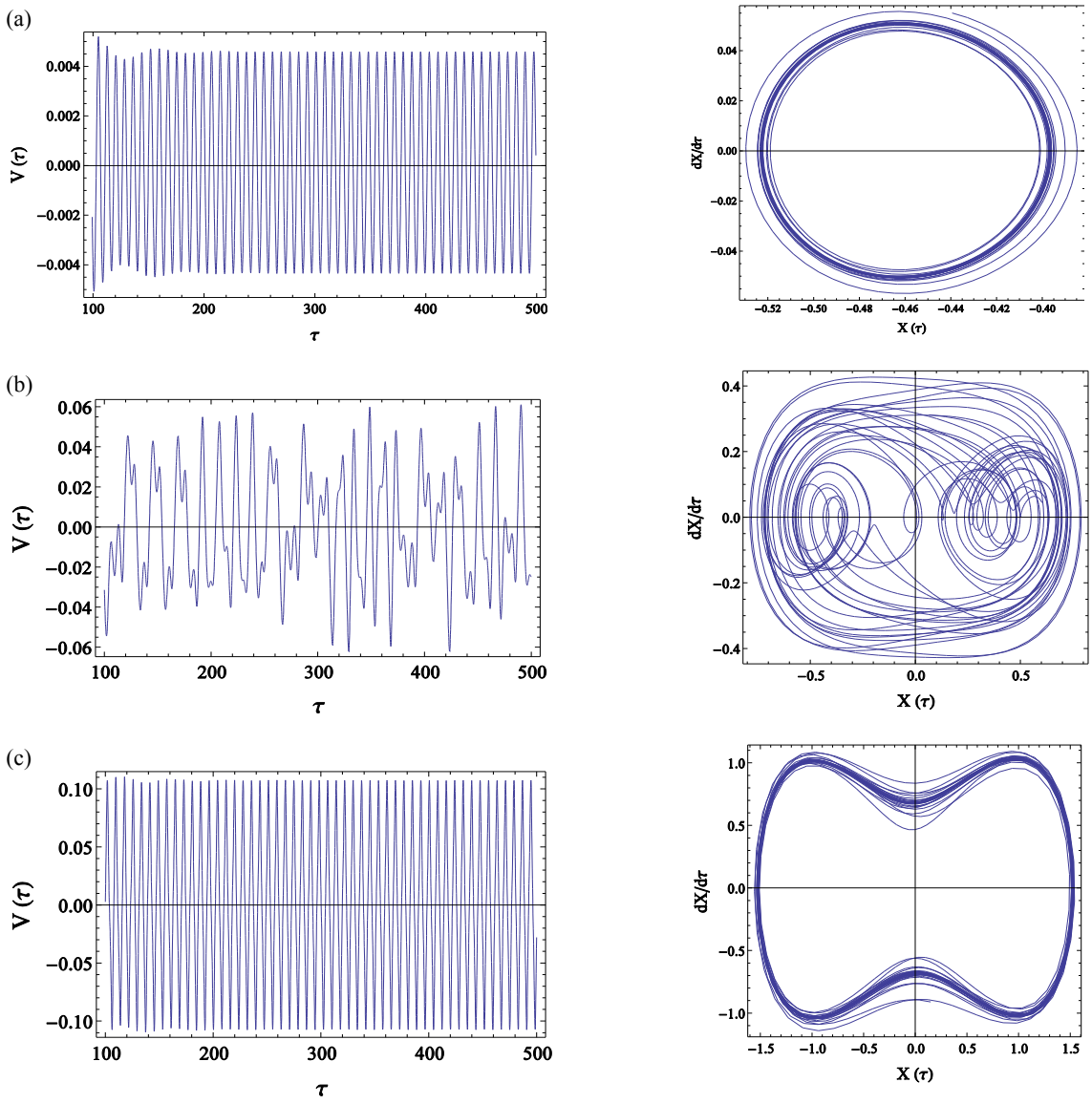

Fig.5
Time response of the harvested voltage and phase portrait diagram of beam tip, when $\Omega = 0.8$. a) f= 0.01, b) f= 0.1, c) f= 1.

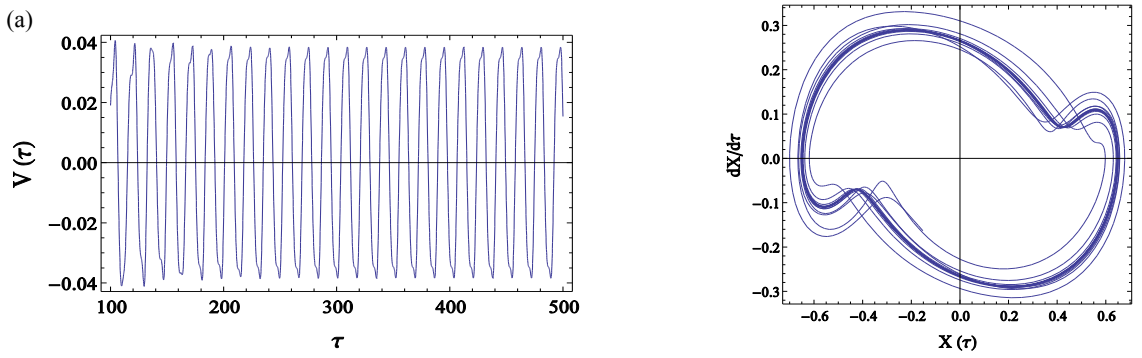

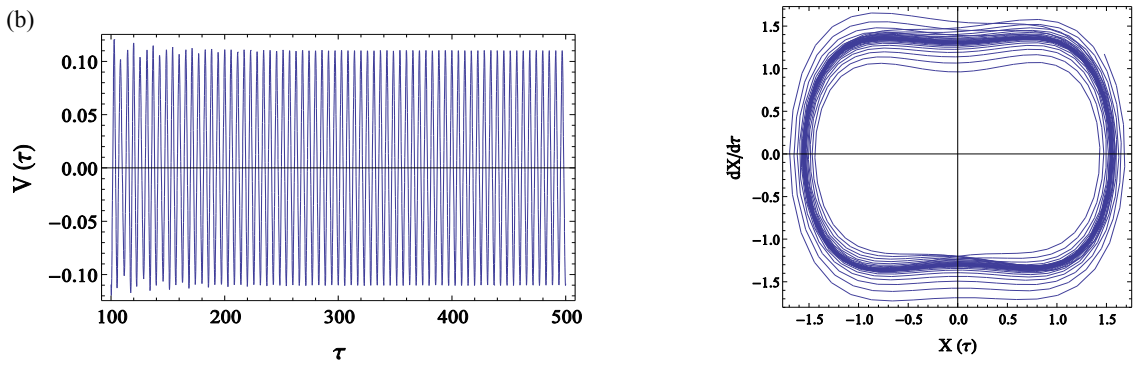

Fig.6
Time response of the harvested voltage and phase portrait diagram of beam tip for f= 0.1. a) $\Omega = 0.1$, b) $\Omega = 0.5$, c) $\Omega = 0.7$.

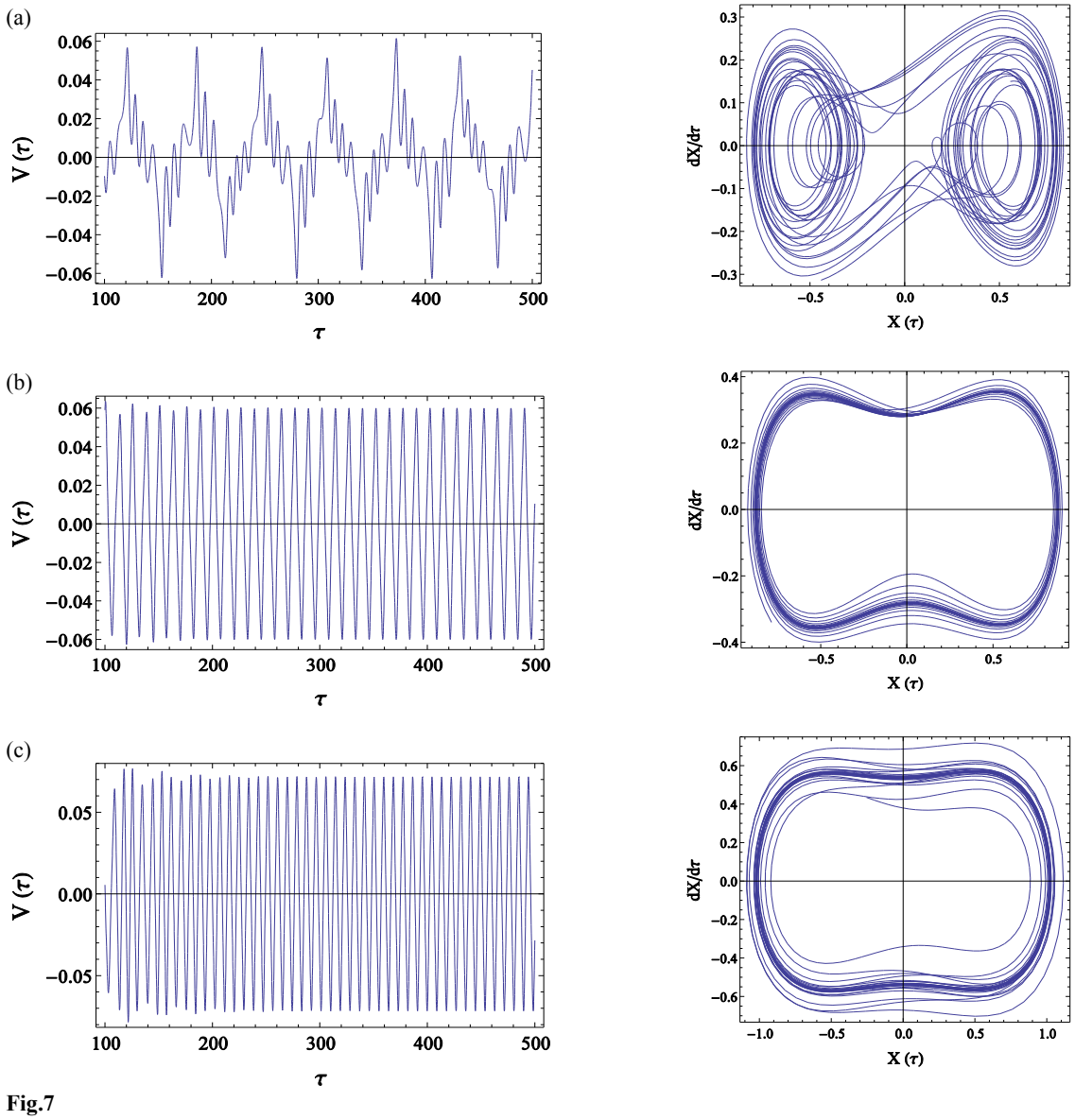

Fig.7
Time response of the harvested voltage and phase portrait diagram of beam tip for $\Omega = 1.1$;(a) f= 0.1, (b) f= 0.5.

4 CONCLUSIONS

Based on the nonlinear vibrational distributed parameter model, the current study analyzed 2-DOF bistable PEH with an elastic substructure in order to amplify the harvesting voltage and broadband the frequency range, considering both nonlinear strains and nonlinear external potential field due to magnetic interaction. Vibrational Analysis of the bistable harvester with high energy inter-well motion was the primary purpose of this research. By tuning the system parameters, such as the mass and stiffness ratios of substructure to the harvester, the magnified excitation level should be expressively reinforced to supply the harvester oscillation and causing both large-amplitude motion and harvested power over broadband frequencies. Also, by raising the elastic substructure stiffness ratio, the harvester oscillations may transform from a low-energy and tight-fitted motion into a bistable and high-energy one that increases the harvesting power. It can be concluded that for PEH, inter-well motion with a high energy level is essential. Also, the other results could summarize as follows:

- ✓ Without an elastic magnifier the low orbit vibrations, cause the intra-well motion and low harvested voltage.
- ✓ By increasing the r_m and r_k of the flexible magnifier, the harvester generates more electrical power.
- ✓ Even by employing a robust elastic substructure, with small the excitation level, the harvested voltage and power were trim.
- ✓ The output voltage and harvested electrical power were chaotic, due to the chaotic motion of the beam tip between two potential wells.

REFERENCES

[1] Talebitooti R., Darvish Gohari H., Zarastvand M., Loghmani A., 2019, A robust optimum controller for suppressing radiated sound from an intelligent cylinder based on sliding mode method considering piezoelectric uncertainties, *Journal of Intelligent Materials Systems and Structures* **30**(20): 3066-3079.

[2] Darvish Gohari H., Zarastvand M., Talebitooti R., Loghmani A., Omidpanah M., 2020, Radiated sound control from a smart cylinder subjected to piezoelectric uncertainties based on sliding mode technique using self-adjusting boundary layer, *Aerospace Science and Technology* **106**: 106141.

[3] Darvish Gohari H., Zarastvand M., Talebitooti R., Shahbazi R., 2021, Hybrid control technique for vibroacoustic performance analysis of a smart doubly curved sandwich structure considering sensor and actuator layers, *Journal of Sandwich Structures and Materials* **23**(5): 1453-1480.

[4] Asadijafari M.H., Zarastvand M.R., Talebitooti R., 2021, The effect of considering Pasternak elastic foundation on acoustic insulation of the finite doubly curved composite structures, *Composite Structures* **256**: 113064.

[5] Hou Y., 2017, Flexible ionic diodes for low-frequency mechanical energy harvesting, *Advanced Energy Materials* **7**(5): 1601983.

[6] Beeby S.P., 2007, A micro electromagnetic generator for vibration energy harvesting, *Journal of Micromechanics and Microengineering* **17**(7): 1257.

[7] Harne R.L., Wang K. W., 2013, A review of the recent research on vibration energy harvesting via bistable systems, *Smart Materials and Structures* **22**(2): 23001.

[8] Aboulfotoh N.A., Arafa M.H., Megahed S.M., 2013, A self-tuning resonator for vibration energy harvesting, *Sensors and Actuators A: Physical* **201**: 328-334.

[9] Bai X., Wen Y., Li P., Yang J., Peng X., Yue X., 2014, Multi-modal vibration energy harvesting utilizing spiral cantilever with magnetic coupling, *Sensors and Actuators A: Physical* **209**: 78-86.

[10] Wu X., Lee D.-W., 2015, Magnetic coupling between folded cantilevers for high-efficiency broadband energy harvesting, *Sensors and Actuators A: Physical* **234**: 17-22.

[11] Daqaq M.F., Bode D., 2011, Exploring the parametric amplification phenomenon for energy harvesting, *Proceedings of the Institution of Mechanical Engineers. Part I: Journal of Systems and Control Engineering* **225**(4): 456-466.

[12] Abdelkefi A., Nayfeh A.H., Hajj M.R., 2012, Global nonlinear distributed-parameter model of parametrically excited piezoelectric energy harvesters, *Nonlinear Dynamics* **67**(2): 1147-1160.

[13] Daqaq M.F., Masana R., Erturk A., Quinn D.D., 2014, On the role of nonlinearities in vibratory energy harvesting : a critical review and discussion, *Applied Mechanics Reviews* **66**(4): 040801.

[14] Yang Z., Zhu Y., Zu J., 2015, Theoretical and experimental investigation of a nonlinear compressive-mode energy harvester with high power output under weak excitations, *Smart Materials and Structures* **24**(2): 25028.

[15] Jahani K., Aghazadeh P., 2016, Investigating the performance of piezoelectric energy harvester including geometrical, damping and material nonlinearities with the method of multiple scales, *Modares Mechanical Engineering* **16**(4): 354-360.

[16] Lin J.-T., Alphenaar B., 2010, Enhancement of energy harvested from a random vibration source by magnetic coupling of a piezoelectric cantilever, *Journal of Intelligent Materials Systems and Structures* **21**(13): 1337-1341.

[17] Zhao D., 2018, Analysis of single-degree-of-freedom piezoelectric energy harvester with stopper by incremental harmonic balance method, *Materials Research Express* **5**(5): 55502.
[18] Tang L., Yang Y., Soh C.K., 2010, Toward broadband vibration-based energy harvesting, *Journal of Intelligent Materials Systems and Structures* **21**(18): 1867-1897.
[19] Tang L., Yang Y., Soh C.-K., 2012, Improving functionality of vibration energy harvesters using magnets, *Journal of Intelligent Materials Systems and Structures* **23**(13): 1433-1449.
[20] Gammaitoni L., Hänggi P., Jung P., Marchesoni F., 2009, Stochastic resonance: a remarkable idea that changed our perception of noise, *European Physical Journal B* **69**(1): 1-3.
[21] Erturk A., Hoffmann J., Inman D.J., 2009, A piezomagnetoelastic structure for broadband vibration energy harvesting, *Applied Physics Letters* **94**(25): 254102.
[22] Ferrari M., Ferrari V., Guizzetti M., Andò B., Baglio S., Trigona C., 2010, Improved energy harvesting from wideband vibrations by nonlinear piezoelectric converters, *Sensors and Actuators A: Physical* **162**(2): 425-431.
[23] Stanton S.C., McGehee C.C., Mann B.P., 2010, Nonlinear dynamics for broadband energy harvesting: Investigation of a bistable piezoelectric inertial generator, *Physica D: Nonlinear Phenomena* **239**(10): 640-653.
[24] Stanton S.C., Owens B.A.M., Mann B.P., 2012, Harmonic balance analysis of the bistable piezoelectric inertial generator, *Journal of Sound and Vibration* **331**(5): 3617-3627.
[25] Karami M.A., Inman D.J., 2011, Equivalent damping and frequency change for linear and nonlinear hybrid vibrational energy harvesting systems, *Journal of Sound and Vibration* **330**(23): 5583-5597.
[26] Erturk A., Inman D.J., 2011, Broadband piezoelectric power generation on high-energy orbits of the bistable Duffing oscillator with electromechanical coupling, *Journal of Sound and Vibration* **330**(10): 2339-2353.
[27] Sebald G., Kuwano H., Guyomar D., Ducharne B., 2011, Simulation of a duffing oscillator for broadband piezoelectric energy harvesting, *Smart Materials and Structures* **20**(7): 75022.
[28] Sebald G., Kuwano H., Guyomar D., Ducharne B., 2011, Experimental duffing oscillator for broadband piezoelectric energy harvesting, *Smart Materials and Structures* **20**(10): 102001.
[29] Kim P., Seok J., 2014, A multi-stable energy harvester: Dynamic modeling and bifurcation analysis, *Journal of Sound and Vibration* **333**(21): 5525-5547.
[30] Zhao D., Gan M., Zhang C., Wei J., Liu S., 2018, Analysis of broadband characteristics of two degree of freedom bistable piezoelectric energy harvester, *Materials Research Express* **5**(8): 085704.
[31] Vasic D., Costa F., 2013, Modeling of piezoelectric energy harvester with multi-mode dynamic magnifier with matrix representation, *International Journal of Applied Electromagnetics and Mechanics* **43**(3): 237-255.
[32] Wang H., Shan X., Xie T., 2012, An energy harvester combining a piezoelectric cantilever and a single degree of freedom elastic system, *Journal of Zhejiang University Science A* **13**(7): 526-537.
[33] Zhou W., Penamalli G.R., Zuo L., 2011, An efficient vibration energy harvester with a multi-mode dynamic magnifier, *Smart Materials and Structures* **21**(1): 15014.
[34] Aldraihem O., Baz A., 2011, Energy harvester with a dynamic magnifier, *Journal of Intelligent Materials Systems and Structures* **22**(6): 521-530.
[35] Aladwani A., Arafa M., Aldraihem O., Baz A., 2012, Cantilevered piezoelectric energy harvester with a dynamic magnifier, *Journal of Vibration and Acoustics* **134**(3): 31004.
[36] Tang L., Wang J., 2017, Size effect of tip mass on performance of cantilevered piezoelectric energy harvester with a dynamic magnifier, *Acta Mechanica* **228**(11): 3997-4015.
[37] Tang L., Yang Y., 2012, A multiple-degree-of-freedom piezoelectric energy harvesting model, *Journal of Intelligent Materials Systems and Structures* **23**(14): 1631-1647.
[38] Wang G.-Q., Liao W.-H., 2016, A bistable piezoelectric oscillator with an elastic magnifier for energy harvesting enhancement, *Journal of Intelligent Materials Systems and Structures* **28**(3): 392-407.
[39] Erturk A., Inman D.J., 2009, An experimentally validated bimorph cantilever model for piezoelectric energy harvesting from base excitations, *Smart Materials and Structures* **18**(2): 25009.